Regenerative Therapy 24 (2023) 311–317

Contents lists available at ScienceDirect

Regenerative Therapy

journal homepage: http://www.elsevier.com/locate/reth

Original Article

Development of new bioabsorbable implants with de novo adipogenesis

Qiannan Zhao [a], Shuichi Ogino [b,*], Sunghee Lee [a], Yuki Kato [c], Yuanjiaozi Li [a], Michiharu Sakamoto [a], Hiroki Yamanaka [a], Takashi Nakano [a], Eiichi Sawaragi [a], Naoki Morimoto [a]

[a] Department of Plastic and Reconstructive Surgery, Graduate School of Medicine, Kyoto University, 54 Shogoin, Kawahara-cho, Sakyou-ku, Kyoto 606-8507, Japan
[b] Department of Plastic and Reconstructive Surgery, Shiga University of Medical Science, Seta Tsukinowa-cho, Otsu, Shiga, 520-2192, Japan
[c] Gunze QOL Research Center Laboratory, 1 Zeze, Aono-cho, Ayabe, Kyoto 623-8511, Japan

ARTICLE INFO

Article history:
Received 7 May 2023
Received in revised form
6 July 2023
Accepted 26 July 2023

Keywords:
Bioabsorbable implant
Adipogenesis
Breast reconstruction
PGA nano sheet
PLLA
Collagen sponge

ABSTRACT

Poly-L-lactic acid (PLLA) mesh implants containing collagen sponge (CS) were replaced with autologous adipose tissue regeneration in vivo. Herein, we investigated the optimal external frames and internal fillings using poly (lactic-*co*-ε-caprolactone) (P (LA/CL)), PLLA, and low-molecular-weight PLLA (LMW-PLLA) as the external frame and polyglycolic acid (PGA) nanosheets and CS as the internal filling. We prepared six implants: P (LA/CL) with PGA nano, PLLA with PGA nano, PLLA with CS, PLLA with 1/2 CS, PLLA with 1/4 CS, and LMW-PLLA with CS, and evaluated adipogenesis at 6 and 12 months using a rat inguinal model. The internal spaces in the P (LA/CL) and LMW-PLLA implants collapsed at 6 months, whereas those in the other four implants collapsed at 12 months. Adipose tissue regeneration was not significantly different between the PLLA-implanted groups at 6 and 12 months and was greater than that in the P (LA/CL) with PGA nano and LMW-PLLA with CS groups. The PGA nanosheet inside PLLA was comparable to the CS inside PLLA in the regeneration of adipose tissue and macrophage infiltration. In summary, PLLA is a promising external frame material in which the internal space can be replaced with adipose tissue. Thus, PGA nanosheets are an alternative internal filling material for adipose tissue regeneration.

1. Introduction

In recent years, the incidence of breast cancer has increased as the most commonly diagnosed malignancy, particularly in young women [1]. Reconstruction after mastectomy can improve self-esteem, body image, and sexual functioning and reduce anxiety and depression [2]. The most common breast reconstruction methods include the use of silicone implants, skin flaps, and autologous fat injections. However, each method has limitations. The use of silicone implants leads to implant-related complications, such as rupture, capsular contracture, and infections [3], and can even result in breast implant-associated anaplastic large cell lymphoma (BIA-ALCL) [4]. Breast reconstruction using an autologous flap may result in abdominal hernia, wound dehiscence, wound infection, and flap necrosis [5], and almost one-third of reconstructive patients require revision surgery [6]. Fat injections require large volumes of autologous fat and repeat procedures owing to the reduced fat retention rate, and the oncological safety and risk of lipofilling oil cysts have been questioned [7,8].

Ectopic fat accumulation in various body parts is often observed in clinical practice [9]. Post-traumatic lipomas occur when cytokines and growth factors produced by local inflammatory tissue after blunt soft tissue trauma lead to the differentiation of preadipocytes into mature adipocytes [9,10]. The infantile hemangioma was replaced with adipose tissue with regression [11]. Based on these observations, we hypothesized that the important factor in adipose tissue regeneration in vivo is to maintain the space to avoid tissue pressure in the long term.

The development of tissue engineering has brought new hope for breast reconstruction. In our previous study, we regenerated

* Corresponding author. Seta Tsukinowa-cho, Otsu, Shiga, 520-2192, Japan.
E-mail address: sogino12@belle.shiga-med.ac.jp (S. Ogino).
Peer review under responsibility of the Japanese Society for Regenerative Medicine.

https://doi.org/10.1016/j.reth.2023.07.008

adipose tissue in a non-bioabsorbable polypropylene (PP) mesh cage filled with a collagen sponge (CS) without the addition of growth factors or adipose stem cells (ASCs) [12]. However, the PP mesh must be removed after the regeneration of adipose tissue. Therefore, a combination of a poly-L-lactic acid (PLLA) mesh and CS was developed as a novel absorbable implant that could regenerate autologous adipose tissue without the addition of ASCs or growth factors [13]. However, the amount of regenerated adipose tissue is small, and we need to investigate superior materials in terms of their adipogenesis ability.

In this study, we used poly (lactic-*co*-ε-caprolactone) (P (LA/CL)), PLLA, and low-molecular-weight PLLA (LMW-PLLA) as the external frame and polyglycolic acid (PGA) nanosheets and CS as the internal filling, and investigated the optimal external frames and internal fillings for adipose tissue regeneration.

2. Materials and methods

2.1. Ethical statement

The animals were maintained at the Laboratory Animal Research Institute, Graduate School of Medicine, Kyoto University, Japan. The number of animals used in this study was kept to a minimum and every effort was made to reduce animal suffering according to the protocol established by the Animal Research Committee of Kyoto University. The experimental protocol was approved by the University Animal Research Committee (license number: Med Kyo 22124).

2.2. Preparation of bioabsorbable implants

We prepared six types of implants with spheroidal prolate shapes: P (LA/CL) with PGA nano, PLLA with PGA nano, PLLA with CS, PLLA with 1/2 CS, PLLA with 1/4 CS, and LMW-PLLA with CS. These implants consist of an external frame and an internal filling material. First, 2–0 PLLA threads and 2-0 P (LA/CL) threads were supplied by Gunze Ltd. (Tokyo, Japan) as the external frame. Next, we prepared PGA nanosheets (NEOVEIL nano®, Gunze Ltd.) and CS with a porosity of 80–95% (PELNAC®, Gunze Ltd.) as internal filling materials. The implants were prepared as described previously [14]. Each columnar mesh (10 mm in diameter and 10 mm in height) was knitted using 2–0 P (LA/CL) and 2–0 PLLA threads. LMW-PLLA implant was prepared by hydrolyzing the 2-0 PLLA columnar mesh for 2 months at 37 °C with phosphate-buffered saline (PBS). Then the top and bottom of the meshes were closed by purse string sutures of the respective thread after tightly packing with a 40 mm × 20 mm × 3 mm CS (PLLA with CS and LMW-PLLA with CS implants), or a 20 mm × 20 mm × 3 mm CS (PLLA with 1/2 CS implant) or a 10 mm × 20 mm × 3 mm CS (PLLA with 1/4 CS implant), or a 44 mm × 44 mm × 0.08 mm PGA nano sheet of the same weight as a 40 mm × 20 mm × 3 mm CS (P (LA/CL) mesh with PGA nano, and PLLA mesh with PGA nano implants). The largest diameter of the short axis was approximately 7.5 mm, while the longest length of the long axis was approximately 18 mm. The gaps between the meshes are squares measuring approximately 1.5 × 1.5 mm.

2.3. Experimental design and operating procedures

Thirty-eight male F344/Jcl rats at 10-week-old were purchased from CLEA Japan (Osaka, Japan). According to standard practice, the rats were anesthetized and maintained by inhalation of isoflurane (Pfizer Inc., Tokyo, Japan). Antibiotics were not administered during the perioperative period. The following procedures were performed on both sides of the inguinal region, and six groups were randomly assigned to each side of each rat. After shaving and depilation, a 2 cm long skin incision was made 5 mm cranially from the inguinal ligament. An incision was made in the inguinal fat pad and a pocket was created to insert the implants. Implants were placed in the pocket above the femoral vessels and fixed to the fat pad using 4-0 nylon sutures (Diadem; Alice Morks Inc., Tokyo, Japan). The fat pad and skin were closed using 4-0 nylon sutures. The number of P (LA/CL) with PGA nano groups, PLLA with PGA nano groups, PLLA with CS groups, PLLA with 1/2 CS groups, and PLLA with 1/4 CS groups was twelve, and the number of LMW-PLLA with CS groups was eight.

2.4. Evaluation of weight and volume of all newly formed tissues

Six or twelve months after implantation, the rats were euthanized using carbon dioxide. All newly formed tissues were harvested from the iliac crest and midline above the muscle layer in the abdominal region and above the muscle layer in the femoral region. The weight of the excised specimen was determined using an electronic balance (PM460; Mettler-Toledo International Inc., Tokyo, Japan), and its volume was determined using a common water displacement approach [15].

2.5. Histological evaluation of the formed tissue inside implants

Harvested specimens were fixed in a 10% formalin neutral buffer solution (FUJIFILM Wako Pure Chemical Industries, Corporation, Osaka, Japan). Each specimen was equally divided into four pieces along the long axis, resulting in three cross-sections. The blocks were embedded in paraffin for hematoxylin and eosin (HE), Azan, and immunohistochemical staining. 3-μm-thick HE-stained sections at the respective three aspect were prepared. A 3-μm-thick Azan-stained section was placed in the central section. HE and Azan staining were performed following standard procedures. All images were captured using a Keyence BZ-X800 (KEYENCE Corp., Osaka, Japan) at × 4 to × 40 magnification. The area of the formed tissue inside the implants and collagen fibers inside the implants were manually measured using the BZ-X800 Analyzer software (Keyence Corp.), and the average area of the three cross-sections of each specimen was used for statistical analysis of the formed tissue inside each implant.

2.6. Evaluation of immunohistochemical staining

Immunohistochemical staining of perilipin was performed to evaluate newly regenerated adipose tissue inside the implants. At the respective three aspect, 3-μm-thick paraffin sections were prepared. After deparaffinization and dehydration, the sections were immersed in antigen inactivation solution (code: 415211; Nichirei Biosciences Inc., Tokyo, Japan) for 20 min at 98 °C in a water bath. After cooling to room temperature, the sections were rinsed with distilled water and soaked in 3% hydrogen peroxide for 10 min at room temperature. The sections were then rinsed twice for 5 min in distilled water and Tris–HCl buffer (containing 0.05% Tween-20 and 0.15 M NaCl) (TBST). To block nonspecific protein binding, sections were immersed in 3% bovine serum albumin (BSA) diluted with PBS for 60 min at room temperature, Rabbit monoclonal antibody (Perilipin-1 [D1D8] XP® Rabbit mAb #9349S; Cell Signaling Technology, Danvers, Massachusetts) at a 1:200 dilution was applied to the sections and incubated overnight at 4 °C. Sections were rinsed in TBST three times for 5 min each. Next, rabbit anti-goat simple stain MAX-PO (Histofine 724142; Nichirei Biosciences Inc., Tokyo, Japan) was applied at room temperature for 30 min. The sections were rinsed again with TBST, exposed to DAB (3-3′-diaminobenzidine–4HCl) (Signal Stain® DAB Substrate Kit

725191; Nichirei Biosciences Inc., Tokyo, Japan), and counterstained with hematoxylin. The area of adipose tissue inside the implants was manually measured using the BZ-X800 Analyzer software (Keyence Corp.). The average area of the three cross-sections of each specimen was used for statistical analysis.

Immunohistochemical staining for anti-CD68 was performed to evaluate pan-macrophage infiltration. At the central aspect, 3-μm-thick paraffin sections were prepared. The staining method followed the process of perilipin staining mentioned above. Rabbit monoclonal antibody (ab125212; Abcam, Cambridge, UK) at a 1:5000 dilution was used as the primary antibody, while simple stain MAX PO was used as a labeled polymer with a secondary antibody. The sections were then exposed to DAB and counterstained with hematoxylin. All images were captured using a Keyence BZ-X800 at × 4– × 40 magnification. The number of macrophages inside the implants was counted using the BZ-X800 Analyzer software (Keyence Corp.). Consistent with our previous findings [16], a threshold was set for the brown tint and the size of individual stained areas, and the regions above this threshold were counted.

2.7. Statistical analysis

All data are expressed as mean ± standard deviation. We used one-way analysis of variance with Bonferroni post-hoc analysis between multiple groups. Statistical significance was set at $P < 0.05$. All statistical analyses were performed using IBM SPSS Statistics for Windows version 28 (IBM Corp., Armonk, NY, USA).

3. Results

3.1. Evaluation of the weight and volume of all the newly formed tissues

No infection was observed during postoperative follow-up. However, one implant was excluded from the LMW-PLLA group at 12 months because of the presence of a tumor (pilomatricoma, variant type) around the implant. The gross appearance of all the newly formed tissues is shown in Fig. 1a. The presence of P (LA/CL), PLLA, and LMW-PLLA threads was confirmed macroscopically for up to 12 months after implantation.

The time courses of the weight and volume of all newly formed tissues are shown in Fig. 1b and c. At six months, the weight and volume of all newly formed tissues were not significantly different among the groups. At 12 months, the weight and volume of the PLLA with 1/2 CS group were greater than those of the PLLA with 1/4 CS and LMW-PLLA with CS groups ($p < 0.01$). The weights and volumes of the PLLA with CS group were greater than those of the PLLA with 1/4 CS group ($p < 0.05$). In addition, the weight and volume of the P (LA/CL) with PGA nano, PLLA with PGA nano, PLLA with CS, and PLLA with 1/2 CS groups at 12 months were greater than those at 6 months ($p < 0.05$).

3.2. Histological assessment of the area of formed tissue and adipose tissue inside implants

Micrographs of the HE-stained sections are shown in Fig. 2a. The P (LA/CL) implants with PGA nano and the LMW-PLLA implants with CS groups collapsed to some extent within 6 months. The internal space in the PLLA group with PGA, CS, 1/2 CS, and 1/4 CS was maintained for up to 6 months but collapsed at 12 months.

The time course of tissue formation inside the implants is shown in Fig. 2b. At six months, the area of the formed tissue in the PLLA with PGA nano, PLLA with CS, PLLA with 1/2 CS, and PLLA with 1/4 CS groups was significantly larger than that in the P (LA/CL) with PGA nano and LMW-PLLA with CS groups ($p < 0.05$). At 12 months, the areas of tissue formed in the PLLA with PGA nano, PLLA with 1/2 CS, and PLLA with 1/4 CS groups were significantly larger than that in the P (LA/CL) with PGA nano group ($p < 0.05$). Moreover, the area of tissue formed at 12 months in the PLLA with PGA nano, PLLA with CS, PLLA with 1/2 CS, and PLLA with 1/4 CS groups was significantly smaller than that at 6 months ($p < 0.05$).

Micrographs of Perilipin-stained sections are shown in Fig. 3a. The time course of the adipose tissue area inside the implants is shown in Fig. 3b and c. At six months, the area of adipose tissue in the PLLA with PGA nano, PLLA with CS, and PLLA with 1/2 CS groups was significantly larger than that in the P (LA/CL) with PGA nano and LMW-PLLA with CS groups ($p < 0.01$). The adipose tissue area in the PLLA with 1/4 CS group was significantly larger than that in the LMW-PLLA with CS group ($p < 0.01$). At 12 months, the PLLA with PGA nano, PLLA with 1/2 CS, and PLLA with 1/4 CS groups were significantly larger than the P (LA/CL) with PGA nano and LMW-PLLA with CS groups ($p < 0.01$). The PLLA with PGA nano group was significantly larger than the PLLA with CS group ($p < 0.05$). Furthermore, the adipose tissue area at 6 months in the PLLA with PGA nano group, PLLA with CS group and PLLA with 1/2 CS group and PLLA with 1/4 CS group was significantly larger than that at 12 months in the corresponding group ($p < 0.05$).

The time course of the percentage of adipose tissue in the tissue formed inside the implants is shown in Fig. 3c. There was no significant difference between the groups at 6 and 12 months or in each group between 6 and 12 months.

3.3. Assessment of collagen fibers inside implants

Micrographs of Azan-stained sections at 12 months are shown in Fig. 4a. Fibrosis was confirmed in the central area of all implants. The areas of the collagen fibers inside the implants were shown in Fig. 4b. The PLLA in the CS group was significantly larger than that in the P (LA/CL) with PGA nano group ($p < 0.05$).

3.4. Assessment of inflammation inside implants

Micrographs of the CD68-stained sections at 12 months are shown in Fig. 5a. Macrophage invasion around the PLLA capsule membrane was confirmed, with an almost complete collapse of the capsule membrane in the P (LA/CL) and LMW-PLLA threads. A small number of macrophages was observed inside the implants. The number of CD68 positive macrophages are shown in Fig. 5b. There was no difference in the number of macrophages between groups.

4. Discussion

Herein, we compared the suitability of several types of external frames and internal filling materials to determine the optimal material for adipogenesis. We confirmed that at both 6 and 12 months after implantation, the PLLA with PGA nano group, PLLA with 1/2 CS, and PLLA with 1/4 CS group showed superior formation of the formed tissue and adipose tissue inside the implants. Implants using PLLA as the external frame material containing PGA nanosheets or CS can maintain internal space and regenerate adipose tissue.

Maintenance of the internal space for a long period is beneficial for adipose regeneration [17,18]. The external frame material is an important factor in the maintenance of the internal space inside implants, for which the internal filling material works supportively [13]. We applied PLLA, P (LA/CL), and LMW-PLLA threads as external frame materials to compare their ability to maintain internal space. PLLA is a biocompatible and biodegradable synthetic polymer that can be safely degraded to lactic acid and has been used in a range of

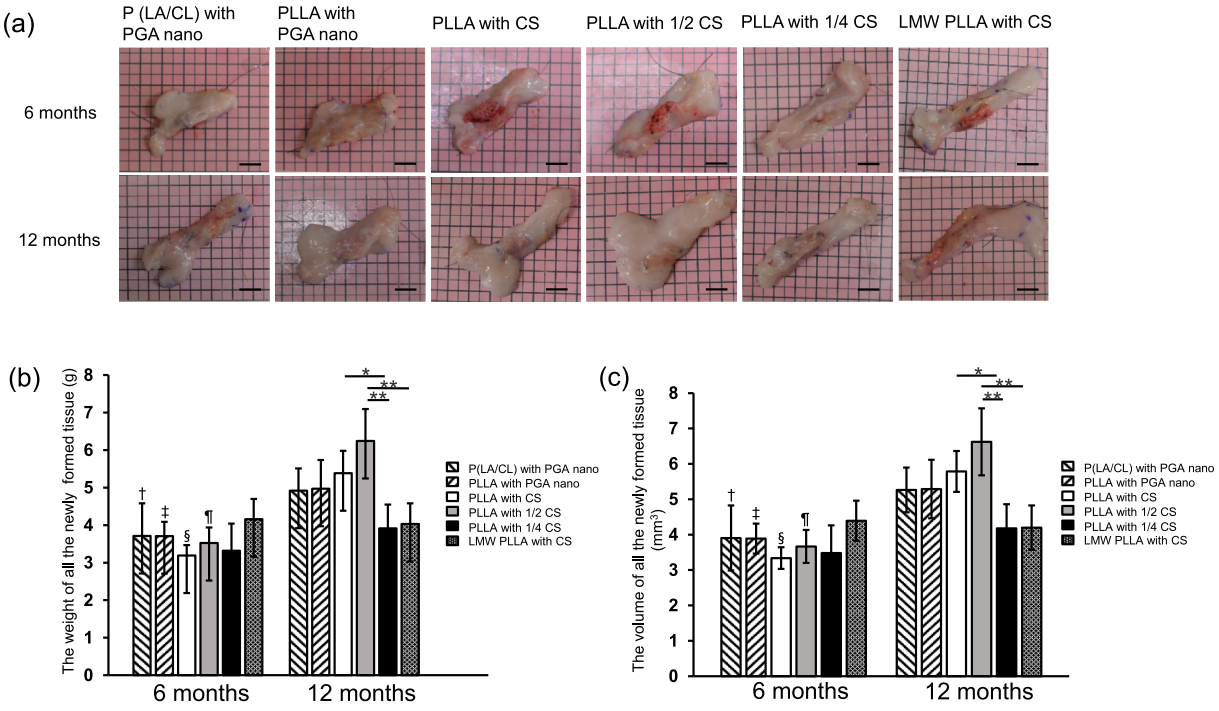

Fig. 1. Weight and volume of all the newly formed tissues. (a) Gross appearance of newly formed tissues. Scale bar: 1 cm. (b, c) Time course of weight and volume of all newly formed tissues. At 12 months, all the newly formed tissues in the 1/2 CS group were significantly larger than those in the CS and 1/4 CS groups. Data are presented as mean ± standard deviation. $*p < 0.05$, $**p < 0.01$, $^{\dagger}p < 0.05$ versus P (LA/CL) with PGA nano group at 12 months, $^{\ddagger, \S, \P}p < 0.01$ versus the corresponding group at 12 months. P (LA/CL): poly (lactic-*co*-ε-caprolactone); PLLA: poly-L-lactic acid; LMW-PLLA: low-molecular-weight poly-L-lactic acid; CS: collagen sponge; PGA nano: polyglycolic acid nanosheets.

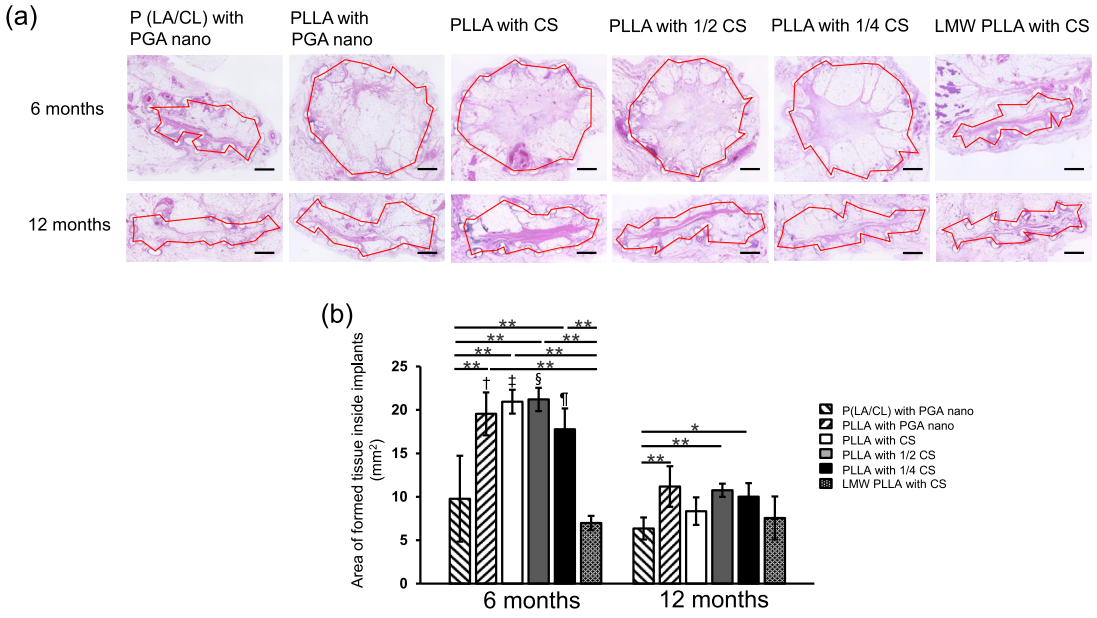

Fig. 2. Micrographs and time course of the formed tissues inside implants. (a) HE-stained sections of tissues formed inside the implants. Red dotted lines indicate the tissue areas formed. The P (LA/CL) and LMW-PLLA groups collapsed after six months. Scale bar: 1 mm. (b) Time course of the tissue areas formed inside the implants. At 6 months, the areas in the four PLLA groups were significantly larger than those in the P (LA/CL) and LMW-PLLA groups. At 12 months, the areas in the PLLA with PGA nano, 1/2 CS, and 1/4 CS groups were significantly larger than that in the P (LA/CL) with PGA nano group. Compared with that at 6 months, the area of the tissues formed inside the implants in the four PLLA groups was significantly smaller at 12 months. Data are presented as mean ± standard deviation. $*p < 0.05$, $**p < 0.01$, $^{\dagger, \ddagger, \S, \P}p < 0.01$ versus the corresponding group at 12 months. P (LA/CL): poly (lactic-*co*-ε-caprolactone); PLLA: poly-L-lactic acid; LMW-PLLA: low-molecular-weight poly-L-lactic acid; CS: collagen sponge; PGA nano: polyglycolic acid nanosheets.

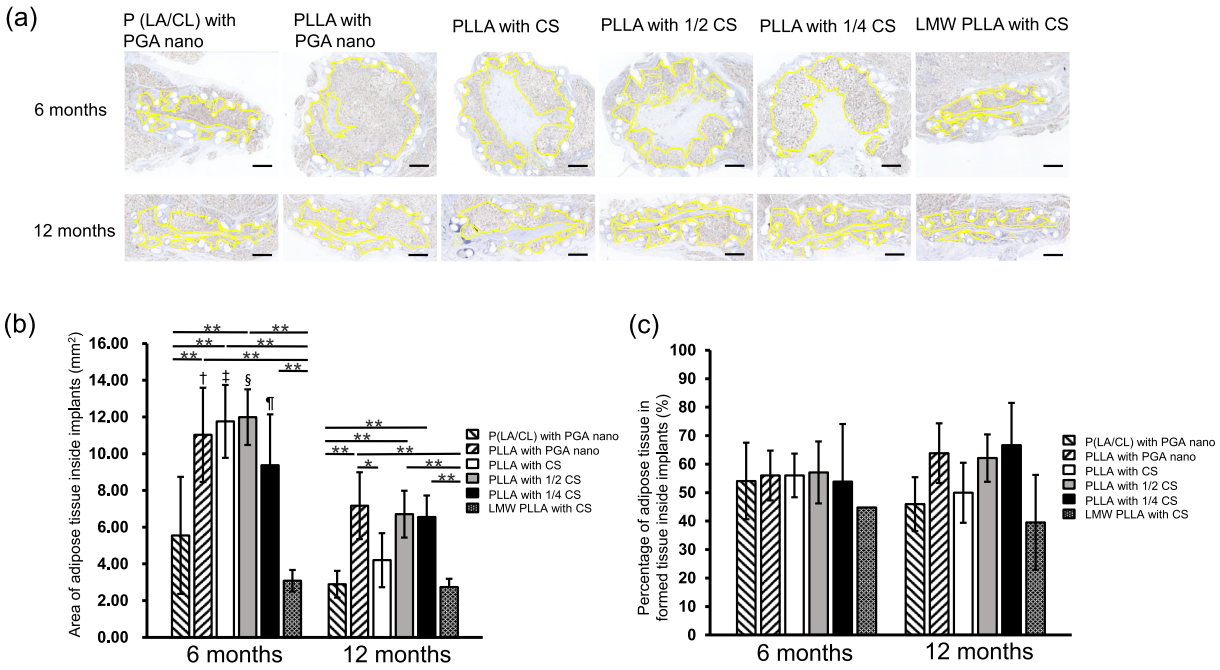

Fig. 3. Micrographs and time course of adipose tissue and the percentage of adipose tissue inside implants. (a) Perilipin-stained sections of adipose tissue inside the implants. The yellow dotted lines indicate adipose tissue areas. Scale bar: 1 mm. (b) Time course of adipose tissue area inside the implants. At 6 months, the areas in the PLLA with PGA nano, CS, and 1/2 CS groups were significantly larger than those in the P (LA/CL) and LMW-PLLA groups. At 12 months, PLLA in the PGA nano, 1/2 CS, and 1/4 CS groups was significantly larger than that in the P (LA/CL) and LMW-PLLA groups. Compared to at 6 months, the area of adipose tissue inside the implants in the four PLLA groups was significantly smaller at 12 months. Data are presented as mean ± standard deviation. $*p < 0.05$, $**p < 0.01$, †, ‡, §, ¶$p < 0.01$ versus the corresponding group at 12 months. (c) Time course of the percentage of adipose tissue inside the implants. No significant differences were observed between the groups. Data are presented as mean ± standard deviation. P (LA/CL): poly (lactic-*co*-ε-caprolactone); PLLA: poly-L-lactic acid; LMW-PLLA: low-molecular-weight poly-L-lactic acid; CS: collagen sponge; PGA nano: polyglycolic acid nanosheets.

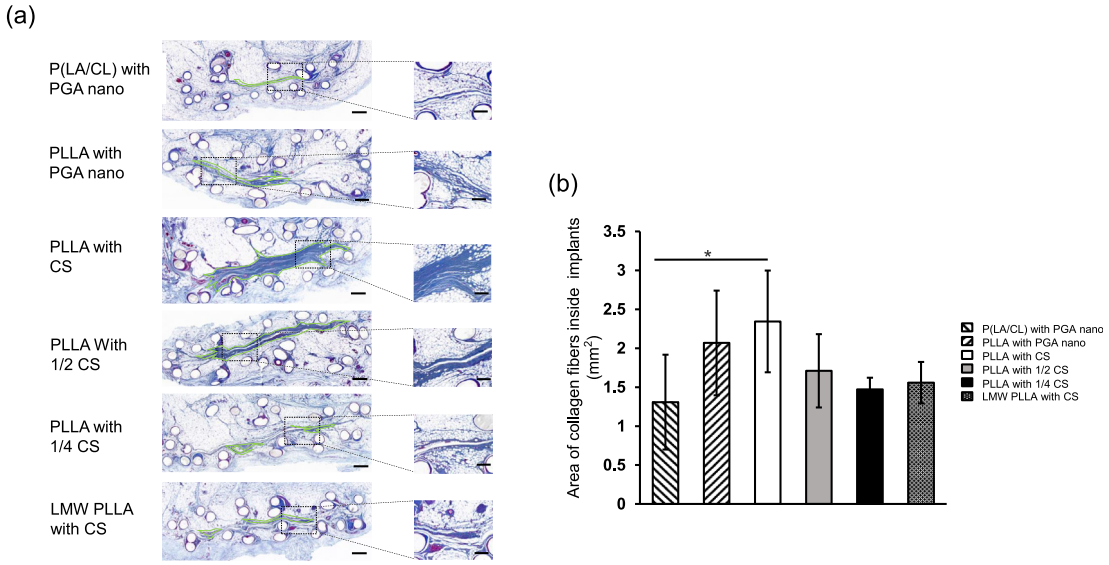

Fig. 4. Micrographs of the collagen fiber area inside implants. (a) Light micrographs of azan staining within the implant at 12 months. Green dotted lines indicate collagen fiber areas. Scale bar:500 μm; Higher magnification scale bar:100 μm. (b) Area of collagen fibers inside the implants. Data are presented as mean ± standard deviation. $*p < 0.05$. P (LA/CL): poly (lactic-*co*-ε-caprolactone); PLLA: poly-L-lactic acid; LMW-PLLA: low-molecular-weight poly-L-lactic acid; CS: collagen sponge; PGA nano: polyglycolic acid nanosheets.

clinical applications for over 30 years [19], including osteochondral lesions [20], lipoatrophy [21], and cosmetic enhancement [22]. P (LA/CL) sutures are characterized by fast absorbance, softness, and high bending plasticity [23]. The LMW-PLLA suture reduces its molecular weight by hydrolysis in PBS, which can be absorbed two months faster than PLLA [24]. The internal space in the groups using PLLA was maintained for 6 months after implantation, but that in the groups using P (LA/CL) and LMW-PLLA collapsed 6 months after implantation (Fig. 2). In addition, although the amount of regenerated adipose tissue in the P (LA/CL) with PGA nano and LMW-PLLA with CS groups was lower than that in the other groups, the adipogenesis ratio inside the implants was the same as that in the other groups (Fig. 3). The tensile strength of PLLA is superior to that of PLACL and LMW PLLA, and its strength half-life is longer compared to PLACL and LMW PLLA [25,26]. This indicates that applying PLLA as an external frame in implants can

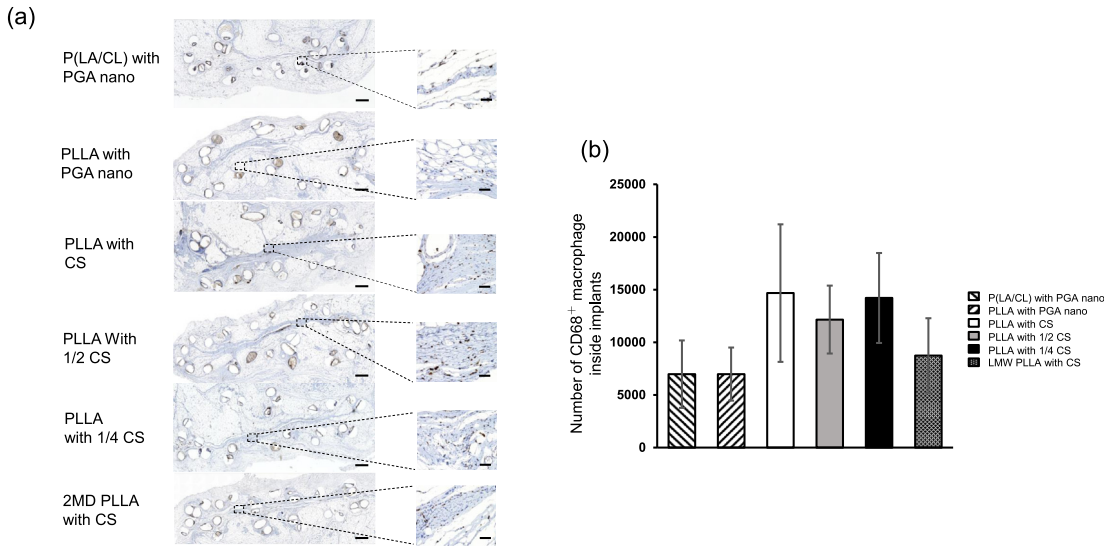

Fig. 5. Micrographs of the $CD68^+$ macrophage count inside implants. (a) Light micrographs of $CD68^+$ macrophages within the implant at 12 months. Scale bar:500 μm; Higher magnification scale bar:50 μm. (b) Number of $CD68^+$ macrophages inside the implants. Data are presented as mean ± standard deviation. P (LA/CL): poly (lactic-*co*-ε-caprolactone); PLLA: poly-L-lactic acid; LMW-PLLA: low-molecular-weight poly-L-lactic acid; CS: collagen sponge; PGA nano: polyglycolic acid nanosheets.

maintain a stronger and more durable internal space over the same period of time. These results indicate that the maintenance of the internal space is an important factor for adipogenesis. PLLA is the preferred material for external frames.

Our previous research indicated that the internal filling material helps induce adipose tissue regeneration using PLLA mesh implants containing CS [13]. CS improves adipose regeneration and helps adipose stem cell attachment and proliferation [27,28]. Collagen sponge supports cell growth and new matrix synthesis, and its porous structure allows cells to easily infiltrate into the scaffold in vivo, which induces new adipose tissue formation [29,30]. However, it has limitations, such as batch-to-batch variation and limited mechanical resistance [31]. In this study, we first used PGA nanosheets as a substitute for the internal filling material for CS in adipose regeneration research. PGA nanosheets are synthetic materials that can be inexpensively manufactured in large quantities without the risk of viruses and other hazards caused by biomaterials [32–34]. The regeneration of adipose tissue in the PLLA with PGA nano group was equal to that in PLLA groups using CS at both 6 and 12 months. At 12 months, fibrosis and inflammation inside the implants in the PLLA with PGA nano group were similar to those in the PLLA groups treated with CS (Figs. 4 and 5). It's reported that PGA contains extra-fine fibers with a large surface area and which results in high cellular characteristics [33]. Therefore, PGA nanosheets are an alternative internal filling material in the de novo adipogenesis.

In other studies, the use of bioresorbable materials to maintain internal space led to adipose tissue regeneration in combination with fat injection [7], growth factors [35], or human umbilical vein endothelial cells [36]. Our implants could regenerate adipose tissue without the addition of growth factors or cells. Furthermore, during the postsurgical follow-up period, neither infection nor hematoma was observed outside or inside the implants, indicating that our implants were safe. Our materials are absorbable, which avoids complications caused by permanent materials, such as BIA-ALCL. In addition, our implants can be made into bioresorbable aggregates that can be reshaped [17]. As a result, the aesthetic needs of breast cancer patients after mastectomy can be met, thereby improving their quality of life.

This study has some limitations. First, the implants collapsed between 6 and 12 months after implantation and could not maintain internal space endurance. Second, the volume of the regenerated adipose tissue was smaller than that of the implants. Therefore, in our next study, we improved the strength of the outside frame to maintain the internal space for a longer period. Furthermore, we investigated the effectiveness of adipogenesis by combining implants with ADSCs to regenerate additional adipose tissue. In addition, we investigated adipogenesis in large animal models using PLLA implants with PGA nano-or CS as internal filling materials to achieve large volumes of de novo adipogenesis.

In summary, PLLA is a promising external frame material in which the internal space can be replaced with adipose tissue. In addition to CS, PGA nanosheets are promising internal filling materials. Implants combined with these materials could be ideal for breast reconstruction without the presence of cells or growth factors.

Ethics statement

The authors confirm that the ethical policies of the journal, as noted on the journal's author guidelines page, have been adhered to, and the appropriate ethical review committee approval has been received.

Declaration of competing interest

All authors declare no conflict of interest in association with the present study.

Acknowledgments

This work was supported by AMED (grant number JP19hm 0102068).

References

[1] Shan Z, Liu L, Shen J, Hao H, Zhang H, Lei L, et al. Enhanced UV resistance role of death domain-associated protein in human MDA-MB-231 breast cancer cells by regulation of G2 DNA damage checkpoint. Cell Transplant 2020;29. https://doi.org/10.1177/0963689720920277.
[2] Richards CA, Rundle AG, Wright JD, Hershman DL. Association between hospital financial distress and immediate breast reconstruction surgery after mastectomy among women with ductal carcinoma in situ. JAMA Surg 2018;153:344–51. https://doi.org/10.1001/JAMASURG.2017.5018.

[3] Prasad K, Zhou R, Zhou R, Schuessler D, Ostrikov KK, Bazaka K. Cosmetic reconstruction in breast cancer patients: opportunities for nanocomposite materials. Acta Biomater 2019;86:41–65. https://doi.org/10.1016/J.ACTBIO.2018.12.024.
[4] Lillemoe HA, Miranda RN, Nastoupil LJ, Clemens MW, Hunt KK. Clinical manifestations and surgical management of breast implant-associated anaplastic large cell lymphoma: beyond the NCCN guidelines. Ann Surg Oncol 2022;29:5722–9. https://doi.org/10.1245/S10434-022-11838-0.
[5] Billig JI, Lu Y, Momoh AO, Chung KC. A nationwide analysis of cost variation for autologous free flap breast reconstruction. JAMA Surg 2017;152:1039–47. https://doi.org/10.1001/JAMASURG.2017.2339.
[6] Finlay B, Kollias V, Hall KA, Clement Z, Bingham J, Whitfield R, et al. Long-term outcomes of breast reconstruction and the need for revision surgery. ANZ J Surg 2021;91:1751–8. https://doi.org/10.1111/ANS.17118.
[7] Chhaya MP, Balmayor ER, Hutmacher DW, Schantz JT. Transformation of breast reconstruction via additive biomanufacturing. Sci Rep 2016;6. https://doi.org/10.1038/SREP28030.
[8] Wederfoort JLM, Hebels SA, Heuts EM, van der Hulst RRWJ, Piatkowski AA. Donor site complications and satisfaction in autologous fat grafting for breast reconstruction: a systematic review. J Plast Reconstr Aesthetic Surg 2022;75:1316–27. https://doi.org/10.1016/J.BJPS.2022.01.029.
[9] Erginöz E, Çavuş GH, Çarkman S. Post-traumatic chest wall lipoma in a violinist: fact or fiction? Interact Cardiovasc Thorac Surg 2022;34:500–1. https://doi.org/10.1093/ICVTS/IVAB266.
[10] Galea LA, Penington AJ, Morrison WA. Post-traumatic pseudolipomas–a review and postulated mechanisms of their development. J Plast Reconstr Aesthetic Surg 2009;62:737–41. https://doi.org/10.1016/J.BJPS.2008.12.021.
[11] Uchiyama A, Tamura A, Etsuko O, Motegi SI, Ishikawa O. Involuted facial infantile hemangioma with fatty replacement successfully treated with surgery. J Dermatol 2014;41:453–4. https://doi.org/10.1111/1346-8138.12457.
[12] Tsuji W, Inamoto T, Ito R, Morimoto N, Tabata Y, Toi M. Simple and long-standing adipose tissue engineering in rabbits. J Artif Organs 2013;16:110–4. https://doi.org/10.1007/S10047-012-0670-4.
[13] Ogino S, Morimoto N, Sakamoto M, Jinno C, Yoshikawa K, Enoshiri T, et al. Development of a novel bioabsorbable implant that is substituted by adipose tissue in vivo. J Tissue Eng Regen Med 2018;12:633–41. https://doi.org/10.1002/TERM.2482.
[14] Ogino S, Sakamoto M, Lee S, Yamanaka H, Tsuge I, Arata J, et al. De novo adipogenesis using a bioabsorbable implant without additional cells or growth factors. J Tissue Eng Regen Med 2020;14:920–30. https://doi.org/10.1002/TERM.3041.
[15] Mian R, Morrison WA, Hurley Jv, Penington AJ, Romeo R, Tanaka Y, et al. Formation of new tissue from an arteriovenous loop in the absence of added extracellular matrix. Tissue Eng 2000;6:595–603. https://doi.org/10.1089/10763270050199541.
[16] Li Y, Sawaragi E, Sakamoto M, Nakano T, Yamanaka H, Tsuge I, et al. Development of gelatin hydrogel nonwoven fabrics (Genocel®) as a novel skin substitute in murine skin defects. Regen Ther 2022;21:96–103. https://doi.org/10.1016/J.RETH.2022.06.002.
[17] Ogino S, Yamada A, Kambe Y, Nakano T, Lee S, Sakamoto M, et al. Preliminary report of de novo adipogenesis using novel bioabsorbable implants and image evaluation using a porcine model. J Artif Organs 2022;25:245–53. https://doi.org/10.1007/S10047-022-01313-8.
[18] Kambe Y, Ogino S, Yamanaka H, Morimoto N, Yamaoka T. Adipose tissue regeneration in a 3D-printed poly(lactic acid) frame-supported space in the inguinal region of rats. Bio Med Mater Eng 2020;31:203–10. https://doi.org/10.3233/BME-201103.
[19] Fitzgerald R, Bass LM, Goldberg DJ, Graivier MH, Lorenc ZP. Physiochemical characteristics of poly-L-lactic acid (PLLA). Aesthetic Surg J 2018;38:S13–7. https://doi.org/10.1093/ASJ/SJY012.
[20] Ikuta Y, Nakasa T, Sumii J, Nekomoto A, Adachi N. Histopathological and radiographic features of osteolysis after fixation of osteochondral fragments using poly-L-lactic acid pins for osteochondral lesions of the talus. Am J Sports Med 2021;49:1589–95. https://doi.org/10.1177/03635465211001758.
[21] Levy RM, Redbord KP, Hanke CW. Treatment of HIV lipoatrophy and lipoatrophy of aging with poly-L-lactic acid: a prospective 3-year follow-up study. J Am Acad Dermatol 2008;59:923–33. https://doi.org/10.1016/J.JAAD.2008.07.027.
[22] Butterwick K, Lowe NJ. Injectable poly-L-lactic acid for cosmetic enhancement: learning from the European experience. J Am Acad Dermatol 2009;61:281–93. https://doi.org/10.1016/J.JAAD.2008.11.881.
[23] Pillai CKS, Sharma CP. Review paper: absorbable polymeric surgical sutures: chemistry, production, properties, biodegradability, and performance. J Biomater Appl 2010;25:291–366. https://doi.org/10.1177/0885328210384890.
[24] Tsuji H, Ikada Y. Properties and morphology of poly(l-lactide) 4. Effects of structural parameters on long-term hydrolysis of poly(l-lactide) in phosphate-buffered solution. Polym Degrad Stabil 2000;67:179–89. https://doi.org/10.1016/S0141-3910(99)00111-1.
[25] Vieira AC, Vieira JC, Ferra JM, Magalhães FD, Guedes RM, Marques AT. Mechanical study of PLA–PCL fibers during in vitro degradation. J Mech Behav Biomed Mater 2011;4:451–60. https://doi.org/10.1016/J.JMBBM.2010.12.006.
[26] Farah S, Anderson DG, Langer R. Physical and mechanical properties of PLA, and their functions in widespread applications — a comprehensive review. Adv Drug Deliv Rev 2016;107:367–92. https://doi.org/10.1016/J.ADDR.2016.06.012.
[27] Kakudo N, Morimoto N, Ogawa T, Taketani S, Kusumoto K. FGF-2 combined with bilayer artificial dermis composed of collagen matrix prompts generation of fat pad in subcutis of mice. Med Mol Morphol 2019;52:73–81. https://doi.org/10.1007/S00795-018-0203-1.
[28] De la Puente P, Ludeña D. Cell culture in autologous fibrin scaffolds for applications in tissue engineering. Exp Cell Res 2014;322:1–11. https://doi.org/10.1016/J.YEXCR.2013.12.017.
[29] Casadei A, Epis R, Ferroni L, Tocco I, Gardin C, Bressan E, et al. Adipose tissue regeneration: a state of the art. J Biomed Biotechnol 2012;2012. https://doi.org/10.1155/2012/462543.
[30] Hiraoka Y, Yamashiro H, Yasuda K, Kimura Y, Inamoto T, Tabata Y. In: In situ regeneration of adipose tissue in rat fat pad by combining a collagen scaffold with gelatin microspheres containing basic fibroblast growth factor, 12; 2006. p. 1475–87. https://doi.org/10.1089/TEN.2006.12.1475. HomeLiebertpubCom/Ten.
[31] Paoletti C, Divieto C, Chiono V. Impact of biomaterials on differentiation and reprogramming approaches for the generation of functional cardiomyocytes. Cells 2018;7. https://doi.org/10.3390/CELLS7090114.
[32] Miyahara E, Ueda D, Kawasaki Y, Ojima Y, Kimura A, Okumichi T. Polyglycolic acid mesh for preventing post-thoracoscopic bullectomy recurrence. Surg Today 2021;51:971–7. https://doi.org/10.1007/S00595-020-02191-4.
[33] Sueyoshi Y, Niwa A, Nishikawa Y, Isogai N. The significance of nanofiber polyglycolic acid for promoting tissue repair in a rat subcutaneous implantation model. J Biomed Mater Res B Appl Biomater 2023;111:16–25. https://doi.org/10.1002/JBM.B.35128.
[34] Kibe T, Koga T, Nishihara K, Fuchigami T, Yoshimura T, Taguchi T, et al. Examination of the early wound healing process under different wound dressing conditions. Oral Surg Oral Med Oral Pathol Oral Radiol 2017;123:310–9. https://doi.org/10.1016/J.OOOO.2016.10.023.
[35] Kimura Y, Tsuji W, Yamashiro H, Toi M, Inamoto T, Tabata Y. In situ adipogenesis in fat tissue augmented by collagen scaffold with gelatin microspheres containing basic fibroblast growth factor. J Tissue Eng Regen Med 2010;4:55–61. https://doi.org/10.1002/TERM.218.
[36] Chhaya MP, Melchels FPW, Holzapfel BM, Baldwin JG, Hutmacher DW. Sustained regeneration of high-volume adipose tissue for breast reconstruction using computer aided design and biomanufacturing. Biomaterials 2015;52:551–60. https://doi.org/10.1016/J.BIOMATERIALS.2015.01.025.